Prediction of Weld Quality in Dissimilar Metal Sheets using Machine Learning Algorithms in R

By

J.I. Onyewudiala

Department of Mechanical Engineering, Imo State University, Nigeria

onyewudialajulius@gmail.com

Abstract

Dissimilar metals with different thicknesses are frequently required due to the increasing demand for lightweight vehicle body constructions. It can be difficult to weld dissimilar metals together because their characteristics change. The purpose of this research is to investigate how welding factors affect the quality and strength of the weld. The Central Campsite Design Matrix was used to perform spot-welding trials on mild steel and 304L SS sheets of varying thickness. The purpose of the study was to determine how the strength of dissimilar metal welds was affected by the weld current, weld time, and weld force. R-language is used to create an empirical relationship for weld strength prediction. To determine which process parameters had a substantial impact on weld strength, ANOVA was used. Analysis is also done on the differences in hardness between the various weld samples. Through confirmatory testing, the ideal weld strength parameters for different sheet thicknesses were confirmed. The study's conclusions offer important new information about how modifications to the weld's characteristics improve the quality of the weld joint.

Keywords: *Tensile strength, resistance spot welding, dissimilar metals, R-programming, and the ANOVA F-test.*

Introduction

The very effective resistance spot welding (RSW) procedure, depicted in Fig. 1, is used in mass manufacturing. With its high speed and ability to be automated with other fabrication processes, it offers the benefits of minimal machine parameter adjustments for the best weldability. RSW is a well-known technique for combining sheet metals that is drawing interest from researchers who want to comprehend its basic properties. Examined and created a correlation between welding parameters and weld strength through statistical analysis [1]. To improve forecast accuracy and make it easier to compare pertinent process parameters, statistical tools such as Factorial Design, 'R' Programming, Taguchi Method, and Response Surface Methodology have been used [2, 3]. Tensile shear strength tests are used to assess the quality of spot weld joints, and welding parameters are taken into account as determinants of weld joint quality.

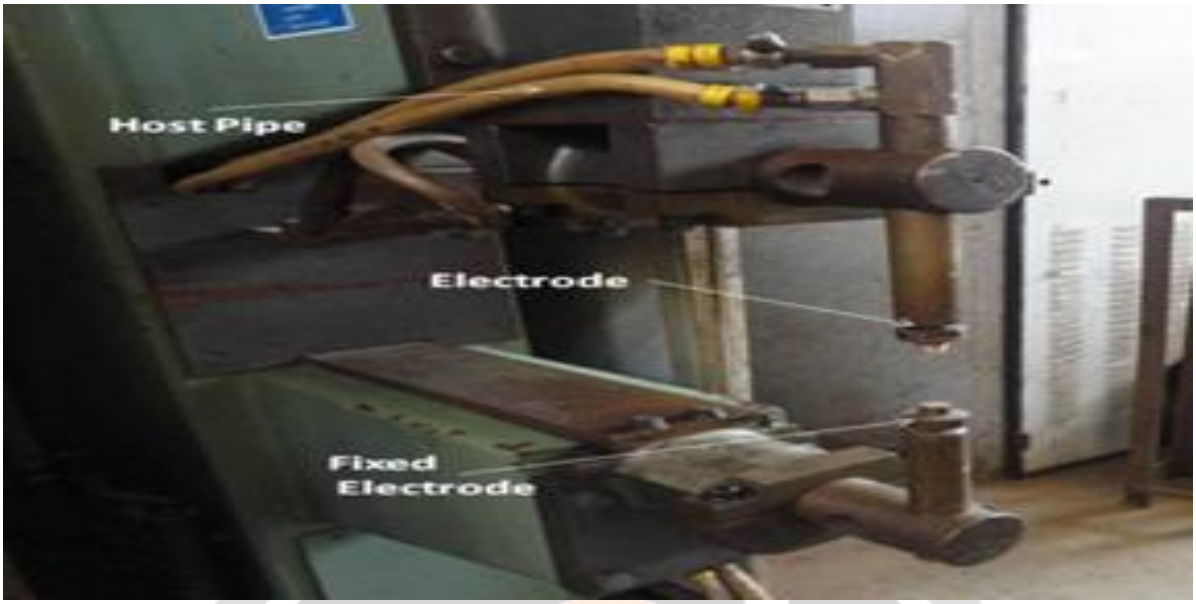

Fig. 1 Resistance spot welding Machine

Initially, a linear regression model was employed, however residuals analysis showed non-linear behavior [4]. In contrast to welding current, which is essential for attaining the best mechanical strength in linked sheets, welding effort and welding time had little effect on mechanical attributes [5]. ANOVA was used to create the empirical relationship, and regression analysis was used to assess the findings. A detailed analysis was conducted to characterize the micro hardness, weld nugget strength, microstructure, and parameter influences on responses [6]. Weld nugget diameter is a crucial factor in optimizing weld strength and fatigue life for aluminum spot welds [7]. Energy input, power, welding speed, beam diameter, angle, etc. are all controlled during the welding process. The experimental and analytical method demonstrated that welding speed and power have a major influence on the weld bead geometry and weld performance [8]. To investigate the effects of process factors, friction stir welding experiments were conducted on comparable aluminum alloys [9–11]. Using the Taguchi Methodology, residual stresses were optimized by determining that feed rate had the greatest impact on longitudinal residual stress and assessing the various kinds of residual stresses that formed in dissimilar metal welds [12, 13]. Design of experiment methodologies are used to develop a semantic framework for predicting the materials' weldability. Common statistical approaches were used for the planning, execution, and analysis [14–17].

According to the literature review above, the authors have experimented with statistical tools and DOE methodologies before. The development of a mathematical model that estimates the best course of action is the main goal of this research. ANOVA is used to predict accuracy in this study, and the examination is also conducted by constructing the "R" computer code to analyze the impact of process parameters on weld strength.

Experimentation

Table 1 provides the chemical composition of base metal 304 ASS and MS sheets (1.0 mm) as determined by the SPRECTOMAX optical emission spectrometer.

Table 1 Chemical Composition

Material	C%	Si%	Mn%	P%	Cr%	S%	N%	Ni%
304 ASS	0.07	0.75	2.0	0.045	18.5	0.030	0.10	8.0 -12
MS	0.08	2.0	0.014	0.009	0.036	0.007	-	0.032

The number of experiments required to fit a quadratic surface and optimize the parameters can be significantly decreased by a well-designed experiment. Eight experiments (corner points) make up the total of 18 experiments in the design. These sites are at the vertices of the cube, and in order to assess pure error, experiments are also conducted four times at the center point. By taking into account parameter choices outside of the process parameter range, the CCD provides quality forecasts across the whole design space. Before the experiment begins, it is acknowledged that CCD can be used to conduct experiments. To guarantee that each coded factor's ± alpha value is provided in Table 2, the factor spacing is decreased. This design incorporates six more tests to add the effect of axial star points in terms of α values. Several blocks are created in order to analyze this data.

Table 2 Experimental factors and their levels for CCD

Factors	Levels of coded variables				
	- α	Low	Medium	High	+ α
	-1.682	-1	0	+1	+1.682
Welding Current (kA)	3.477	6.000	7.500	9.000	11.523
Weld time (Cycle)	6.59	15.00	20.00	25.00	33.41
Electrode Force (kN)	0.477	3.000	4.500	6.000	8.253

One useful parameter for forecasting how a material will behave under various stress scenarios is its tensile strength. The deformation and stresses that a material can tolerate are used to gauge its strength. Water jet machining was used to cut the test specimen in Figure 2 in accordance with ASTM E8 standards.

Fig. 2 Universal Tensile Strength (UTS) Machine and Specimen

The FIE brand, UTN-40, 400 kN Capacity equipment was used to test the weld specimens for Ultimate Tensile Strength (UTS). During UTS testing, the weld center line is positioned perpendicular to the loading axis. The specimens' fracture positions and UTS results are displayed in Table 3. The specimens are prepared for microstructural analysis after being sliced and washed with a solution of NaOH and H_2SO_4.

Table 3: Weld Strength results as per CCD

Sr. No.	Welding Input Process Parameters			Response
	Current (kA)	Time (Cy)	Force (kN)	Weld strength (kN)

1	6.000	15.00	3.000	5.12
2	9.000	15.00	3.000	4.87
3	6.000	25.00	3.000	5.09
4	9.000	25.00	3.000	4.84
5	6.000	15.00	6.000	5.26
6	9.000	15.00	6.000	5.01
7	6.000	25.00	6.000	5.23
8	9.000	25.00	6.000	4.97
9	3.477	15.00	4.500	4.80
10	11.523	15.00	4.500	5.57
11	7.500	6.59	4.500	5.12
12	7.500	33.41	4.500	5.01
13	7.500	20.00	0.477	4.62
14	7.500	20.00	8.253	5.17
15	7.500	20.00	4.500	5.04
16	7.500	20.00	4.500	5.04
17	7.500	20.00	4.500	5.04
18	7.500	20.00	4.500	5.04
Average Weld Strength				5.04

Development of Mathematical Model

Figure 3 illustrates the process for creating code that uses R-programming to estimate response based on input parameters. Based on R2 and P-value, power polynomial regression is used for Block I, II, and Total. This determines which block fits the data the best and provides the mathematical model in the form of a power polynomial equation that is created using the tensile strength data of different thick sheets.

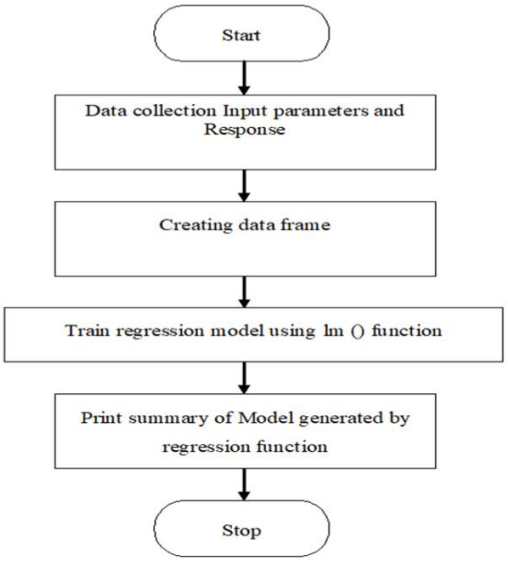

Figure 3 Flow chart identifying best fitted block

Table 4 and Equation (4) provide the results of R-Programming for Block I.

Block1. Lm = ws1.0block_1~wc1.0block_1+wt1.0block_1+wf1.0block_1, data = d1.0block_1 (4)

Table 4: Results of Block_1

1	2	3	4	5	6	7	8	9
-0.051	0.0145	-0.022	0.0144	0.0939	0.0723	-0.035	-0.028	-0.028

Coefficients

Parameters	Estimate	Standard Error	t-Value	Pressure
Intercepts	5.689919	0.141545	40.199	0.000007
Wc1,0block_1	-0,093009	0.009952	-9.346	0.000236
Wt1,0block_1	-0.006695	0.003968	-1.687	0.152344
Wf1,0block_1	0.046667	0.021336	2.187	0.080375

The F-statistic is 31.66 on 3 and 5 DF, the p-value is equal to 0.00112, the residual standard error is 0.06401 with 5 degrees of freedom, and the Multiple R2 value is 0.95 and Adjusted R2 is 0.92. Block I is the most significant, as determined by the ANOVA table and p-value, and is shown in eq. (1).

$$\boldsymbol{Y = 5.6899 - 0.093009X_1 - 0.006695X_2 - 0.046667X_3} \quad (1)$$

In this case, Y represents the response, X1 represents the weld current, X2 represents the weld duration, and X3 represents the electrode force or weld force. Equation (2) and Table 5 provide the results of R-Programming for Block-II.

Block 2.Lm = ws1.0block_2 ~ wc1.0block_2+ wt1.0block_2+wf1.0block_2, data = d1.0block_2. (2)

Table 5: Results of Block 2

1	2	3	4	5
-0.007	-0.012	0.0152	0.01	0.0939
6	7	8	9	
0.0034	-0.277	0.280	-0.006	
		Coefficients:		
Parameters	Estimate	Standard Error	t-Value	Pressure
Intercepts	5.576862	0.511703	10.899	0.000113
Wc1,0block_2	-0,08500	0.058885	-1.443	0.208481
Wt1,0block_2	-0.003048	0.011258	-0.271	0.797429
Wf1,0block_2	0.037274	0.0301	1.241	0.269564

The F-statistic is 1.213 on 3 and 5 DF, the p-value is equal to 0.3957, the multiple R2 value is 0.8211, the adjusted R2 is 0.7382, and the standard residual error is 0.1767 with 5 degrees of freedom. The equation is as follows when the numbers are rounded to three decimal places:

$$\boldsymbol{Y = 5.689 - 0.093X_1 + 0.0066X_2 - 0.0466X_3} \quad (3)$$

Equation (4) provides the outcome of R-Programming for Total Block.

Total Block.Lm = ws1.0_total_block~ wc1.0_total_block + wt1.0_total_block + wf1.0_total_block, data = d1.0_total_ block (4)

The following is the result of R-Programming for Total block, lm.

Min	IQ	Median	3Q	Max
-0.1762	-0.01177	-0.00235	-0.03019	0.1259
		Coefficients:		
Parameters	Estimate	Std, Error	t- value	Pr
Intercepts	5.569267	0.110715	50.303	1.0x10-6
Wc1.0_total_block_2	-0,091434	0.010419	-8.776	0.000459
Wt1.0_total_ block_2	-0.005913	0.003071	-1.925	0.0747
Wf1.0_total_ block_2	0.061928	0.01065	5.815	0.0000449

As a result, the Block value and response are more correlated in this case. R on 3 and 5 DF, the p-value is equal to 0.00112, the F-statistic is 31.66, the Multiple R2 value is 0.95, and the Adjusted R2 is 0.92. Equation (5) provides the power law equation that was constructed.

$$WS = 5.5639I^{-0.92}T^{0.0059}F^{-0.061} \quad (5)$$

4.0 Results and Discussion

The findings from the investigation of the mathematical models for the strength, optimality, and Pareto chart major effect plots are described. Surface plots are used to illustrate the in-depth talks of how the parameters interact with the answers.

4.1 Actual vs. predicted weld strength scatter plot

As seen in figure 4, the scatter diagram displays the values of the weld strength derived from experimentation and the R programming model. The R2 score is 95.63%, indicating that the projected outcomes are more accurate than the real, with an average variation of 0.02 kN between the two.

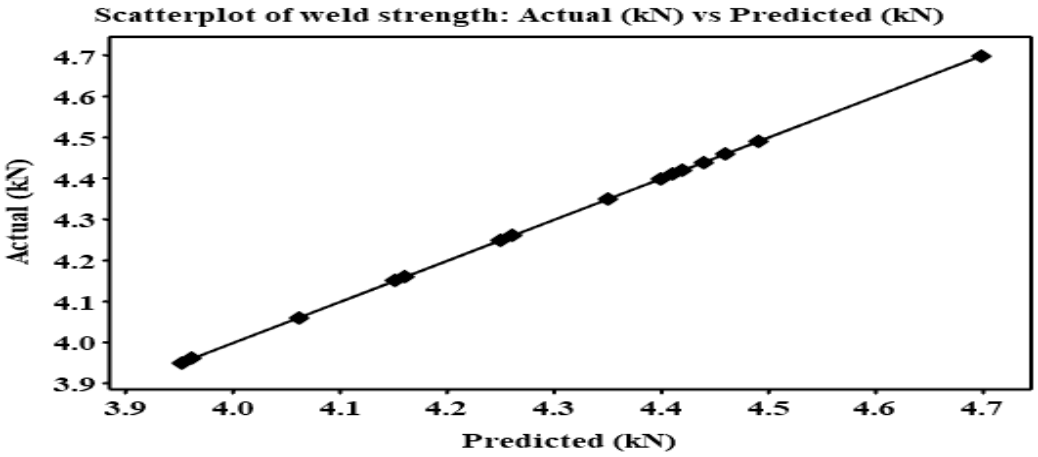

Fig. 4 Actual vs Predicted weld strength

4.2 Main effect plot for the weld strength

The key effects of each parameter on thickness are depicted in the main effects plot of weld strength in Figure 4. When compared to other factors, the main effect plot demonstrates the significant impact of weld current. In particular, an increase in weld strength is correlated with an increase in current supply. Furthermore, it is shown that weld time has a moderate impact on strength, with strength initially increasing as weld time increases up to a specific threshold, after which weld force starts to drop and weld strength starts to decline.

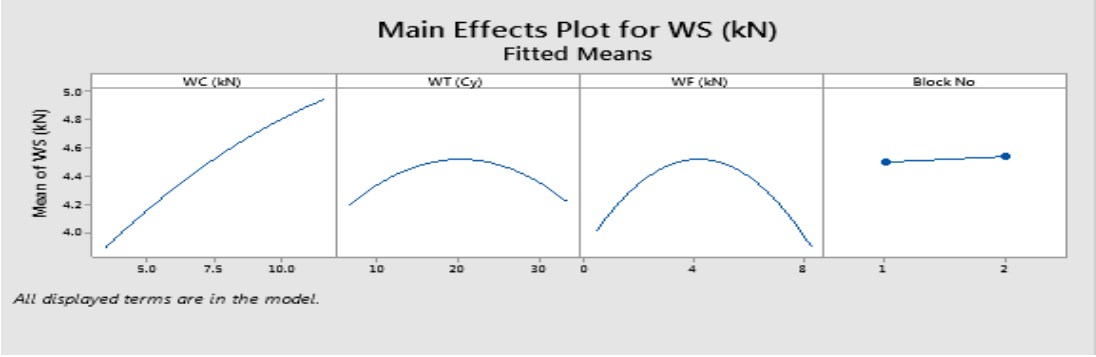

Fig. 5 Main effect plot for the weld strength

4.3 Normal Probability plots for tensile shear strength

The graphs derived from the ANOVA findings, which include several kinds of fits and interactions within the created model, show the relevance of the regression. As seen in Figure 6, which shows normal probability charts for the sheet's strength, the generated mathematical models are verified using residual plots. A normal distribution of errors is indicated by the residuals' alignment with a straight line in these graphs. To measure how close anticipated and experimental values are to one another, the coefficient of determination, or R2, is utilized. The statistical model that has been developed for strength has an R2 value that is higher than 95%.

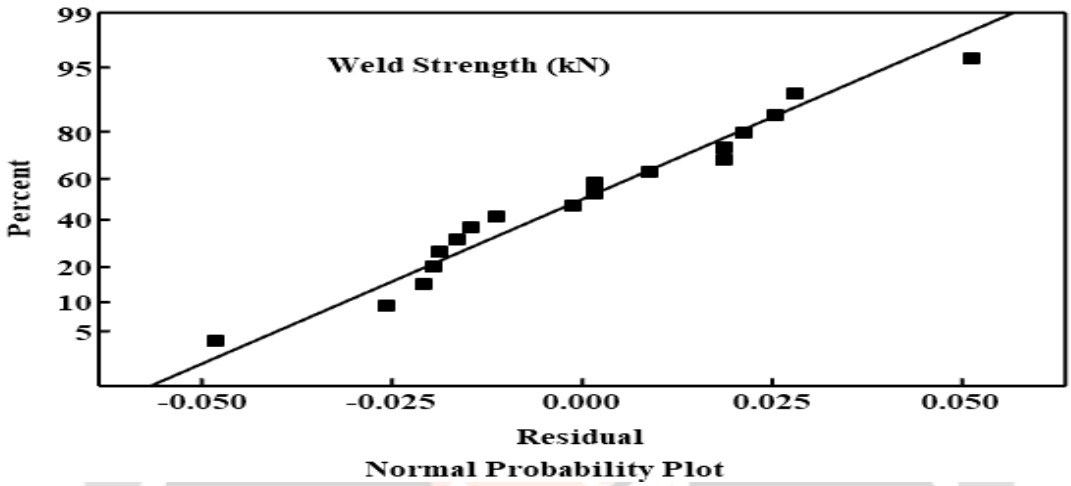

Fig. 6 Normal Probability Plot for tensile-shear strength

4.4 Pareto Analysis

A Pareto chart showing the absolute values of standardized impacts ranked from largest to smallest is shown in Figure 7. The null hypothesis is tested using these standardized effects, which are shown by t-statistics. A reference line is used in the chart to indicate statistically significant effects. Interestingly, bars that cross the reference line in the Pareto graphic are considered statistically significant. The statistical significance at the 0.05 level is indicated by the fact that factor A and the interaction of the CC and AB factors clearly cross the reference line at 2.78. Factors A, CC, and AB clearly have a significant impact on the response, according to the Pareto chart.

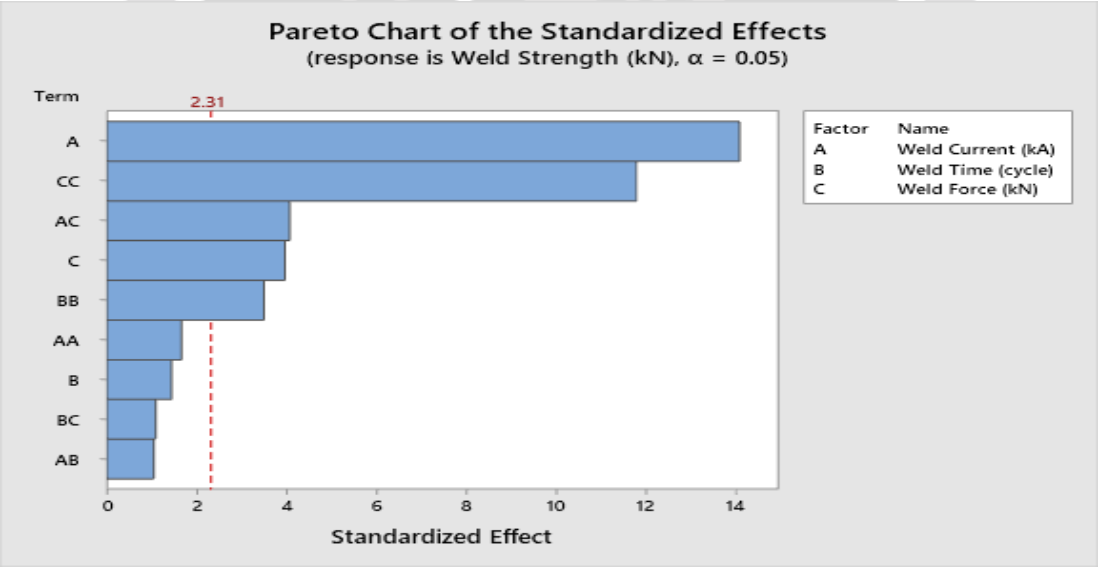

Fig. 7 Pareto analysis plots for tensile-shear strength

4.5 Response Optimization of weld Strength

Figure 8 shows the primary effects of various process factors on the weld strength of a sheet that is 1.0 mm thick, as predicted by the mathematical model. Figure 8 illustrates how current affects weld strength for spot welds. As weld current increases, a maximum weld strength of 4.95 kN is achieved at current (11.53 kA). This is because an increase in weld current causes heat to be generated in the weld, which in turn causes the penetration depth to increase.

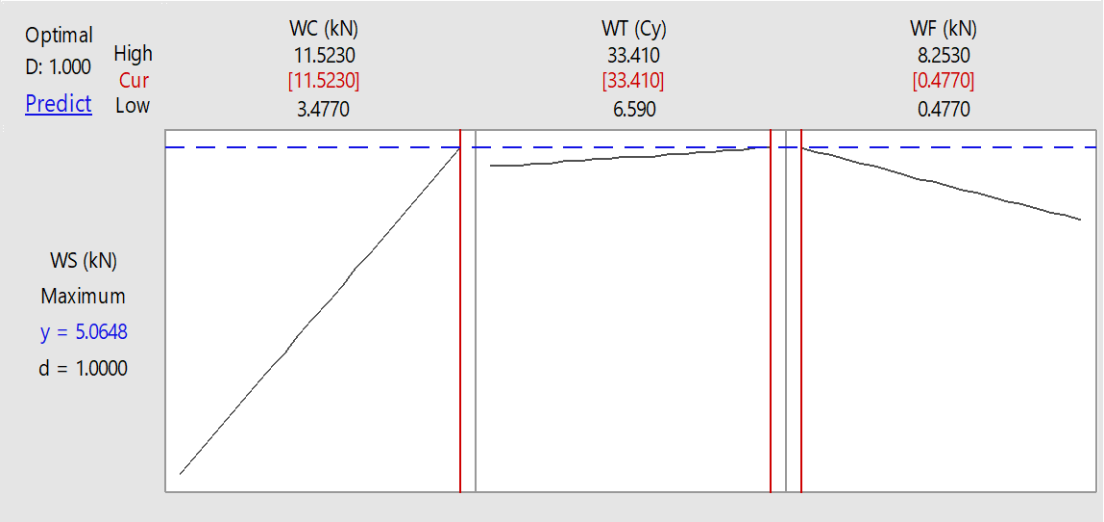

Fig. 8 Response Optimization

Figure 7 illustrates how weld time affects weld strength, showing that spot weld strength rises as weld time increases. At 32.05 cycles of weld duration, the maximum weld strength of 4.95 kN is achieved. According to Joule's law, the rationale for achieving more strength increases as welding duration increases. The maximum joint strength of 4.95 kN is achieved at an electrode force of 6.13 kN, after which it starts to decline. The effects of electrode forces on weld strength reduced as the weld force increased. This is because an increase in electrode force raises the heat energy, which lowers the weld nugget's electrical resistance.

Thus, Figure 7 shows the primary effects of various process parameters on the weld strength of a sheet that is 1.0 mm thick, as predicted by the mathematical model. Figure 8 illustrates how current affects weld strength for spot welds. As weld current increases, a maximum weld strength of 4.95 kN is achieved at current (11.53 kA). This is because an increase in weld current causes heat to be generated in the weld, which in turn causes the penetration depth to increase.

4.6 Contour plots of Models

The quality engineer can determine the ideal process parameters with the help of the contour plots, which offer information about the interaction of input and response parameters that is highly relevant. The weld current versus weld time counter graphs in Figure 9 demonstrate that low weld current (10 kA) results in low weld strength (4.0 kN) at lower weld times (12 cycles). Maximum weld strength (4.6 kN) is obtained with ideal weld current (11.53 kA) and weld time (20 cycle). In line with Joule's law, weld strength increases as weld current increases because heat generated by current causes the temperature to rise, which in turn affects weld size and strength. Furthermore, compared to weld duration, weld current is more susceptible to variations in weld strength.

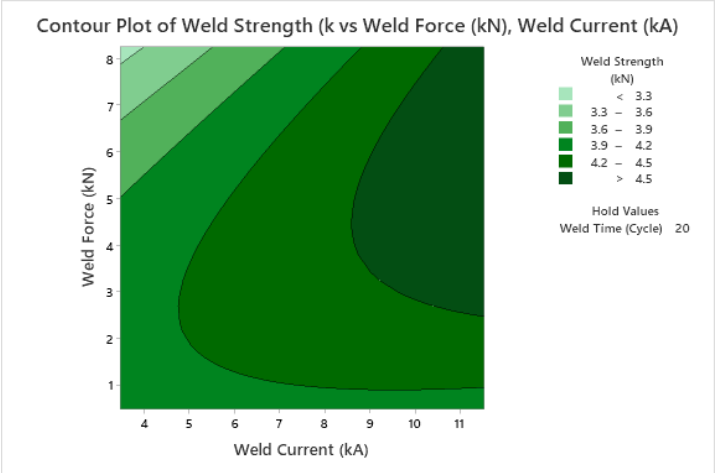

Fig. 9 Contour plots of weld strength

The weld strength obtained for the variation of current from 4.0 kA to 12.0 kA and the electrode force from 1.0 kN to 8.0 kN is depicted in the contour plots in Figure 10. At a constant weld duration (20 cycles), the increased strength is achieved with a lower force and a higher current. Additionally, it is discovered that the highest weld strength of 4.5 kN is achieved at weld forces of 2.5 kN to 8 kN and weld currents of 9 kA to 11.53 kA. As the current and electrode force grow, the greater current compensates for the increased weld force, which results in less welding heat. According to the contour plot, a particular weld strength feature can be achieved by using a weld mode at a particular combination of process parameters. Based on production demands, the contour plots give production direction for determining the right process parameters to achieve the specified weld strength.

Figure 11 shows the contour plots of the measured weld strength vs the weld duration and force. When the weld time was increased from 18 to 28 cycles and the electrode force was increased from 3 to 4.5 kN, the contour lines of the expected weld strength values increased from 3.9 to 4.4 kN. While weld force has a negative impact on weld strength for a fixed current value (7.5 kA), weld time has a positive influence on strength.

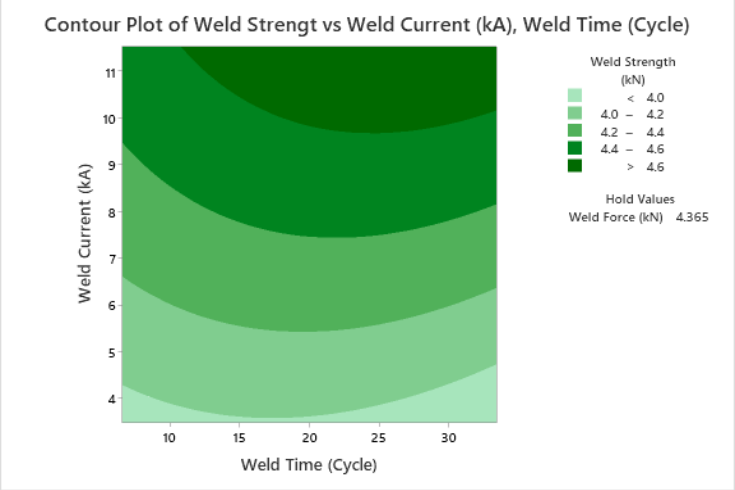

Fig. 10 Contour plots of weld strength

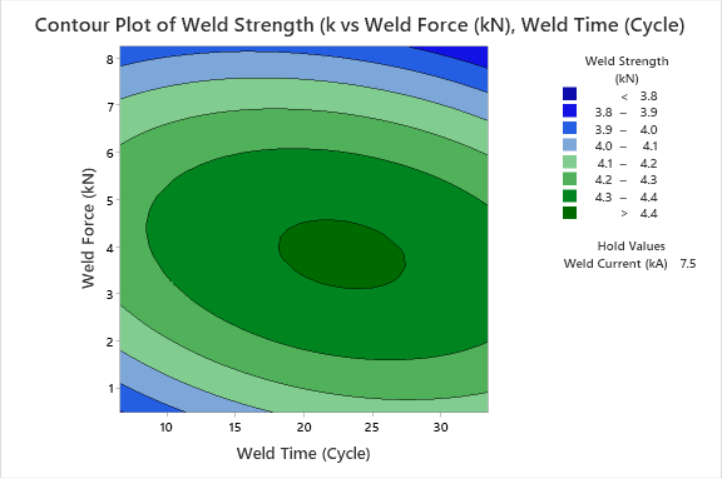

Fig. 11 Contour plots of weld strength

Strength increases more suitably as the weld time increases because more heat builds up in the weld area. Conversely, better heat dissipation, a wider contact area, and less contact resistance are produced by a larger weld force. Therefore, a significantly longer welding time combined with a lower electrode force may result in the best welding procedure. Weld time is more sensitive to strength than weld force, when compared to both weld time and weld force at a constant 7.5 kA weld current.

4.7 Micro hardness measurements

The micro-hardness values acquired from the automated micro-hardness measurement machine on the weld nugget's flanks are shown in Figure 12. It is discovered that the ASS HAZ side's hardness value is lower than the MS side's. The micro-hardness values show a rise to 394 VHN within the weld nugget region. Although the micro-hardness distribution seems to be uniform throughout the weld nugget region, the MS side exhibits a higher hardness—more precisely, 15 VHN more. This discrepancy is explained by increased melting as opposed to the ASS (304) plate, which causes a quicker cooling process.

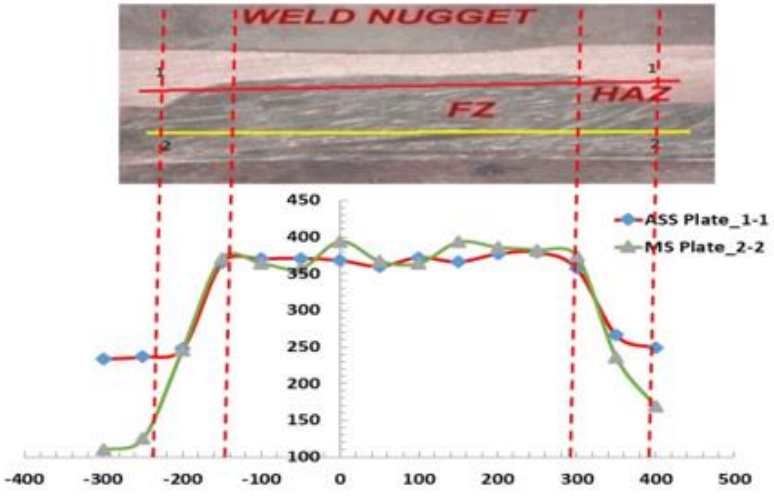

Fig. 12 Weld hardness variation in weld nugget

5.0 Conclusion

The possibility of dissimilar metal RSW of thin sheets of 1.0 mm is revealed by the CCD investigation; the mathematical model was created using the "R" programming language. The following are the findings from this investigation:

1. Clamping force has the least impact on weld strength and nugget diameters, while weld current has the greatest.
2. Using the experimental data gathered, a Central Composite Design of 18 trials was used to examine the effects of force, time, and current at two levels each. The established mathematical model showed that, within the range of parameters of the procedure chosen for welding thin sheets, the weld strength was more than 95% accurate.
3. ASS 304 and mild steel have base metal tensile strengths of 5.10 kN and 4.10 kN, respectively. But the weld strength is 5.57 kN, which means it is 9.21% stronger than ASS 304, while mild steel sheet has a weld strength of 35.80%.
4. The weld strength of 5.0648 kN, which was 26.62% higher than mild steel and 0.69% lower than austenitic stainless steel, is shown in the weld joint made at ideal input process parameters (11.53 A weld current, 33.41 Sec weld duration, and 0.477 kN).
5. The weld nugget's micro hardness on the MS side is 4.09% lower than on the ASS side.

References

[1] De, O. P. Gupta, L. Dorn, An Experimental Study of Resistance Spot Welding in 1 mm Thick Sheet of Low Carbon Steel, Proc lnstn Mech Engrs Vol 210, IMechE 1996 pp 341-347.

[2] W. M. Thomas, D. G. Staines, P. J. Oakley, E. R. Watts, Friction stir welding for aluminum applications process development, in: Proceedings of the 5th International Forum on Aluminum Ships, 2005, pp. 137–144.

[3] D. Nataliia, G. Erik, Z. Igor, Z. Klaus, Mathematical modelling of friction stir welding considering dry and viscous friction, Appl. Math. Model. 67 (2019) 1–8.

[4] Hamidinejad S.M., Kolahan F., Kokabi A. H., The modeling and process analysis of resistance spot welding on galvanized steel sheets used in car body manufacturing. Mater Design 34 pp 759–767(2012).

[5] J. B. Shamsul and M. M. Hisyam, "Study of Spot Welding of Austenitic Stainless Steel Type 304," J. Appl. Sci. Res., vol. 3, no. April, pp. 1494–1499, 2014.

[6] A. K. Biradar, B. M. Dabade "Optimization of resistance spot welding process parameters in dissimilar joint of MS and ASS 304 sheets" Materials Today proceedings, Elsevier Publication,26 (2020) 1284 – 1288.

[7] P. H. Thornton, A.R. Krause and R. G. Davies "The aluminum spot weld' Welding Journal 75-3 1996 pp 101s-108s

[8] A. P, Tadamalle, Y. P., Reddy, E. Ramjee "Influence of laser welding process parameters on weld pool geometry and duty cycle" Advances in Production Engineering and management, Volume 8, 2013, pp 52–60.

[9] Ankur Gill, Dhiraj Parkash Dhiman, Sandeep Sharma, Mathematical modeling of process parameters of friction stir welded aluminium alloy joints using central composite design, Mater. Today: Proc. 5 (14 Part 2) (2018) 27865– 27876.

[10] Yashar Javadi, Seyedali Sadeghi, Mehdi Ahmadi Najafabadi, Taguchi optimization and ultrasonic measurement of residual stresses in the friction stir welding, Mater. Des. 55 (2014) 27–34.

[11] A P. Tadamalle, Y. P. Reddy, E. Ramjee, K.V.K. Reddy, Evaluation of Nd: YAG Laser Welding Efficiencies for 304L Stainless Steel, Procedia Materials Science, 6, 2014, 1731-1739.

[12] A. P. Tadamalle, Y. P. Reddy, E. Ramjee, V. K. Reddy, Influence of welding speed on the melting efficiency of Nd: YAG laser welding, Advances in Production Engineering & Management 9 (3), 1013, 128-136

[13] Kyoung-Yun Kim, Fahim Ahmed "Semantic Weldability Prediction with RSW Quality" 2018 published by Elsevier.

[14] A. P. Tadamalle, Y. P. Reddy, E. Ramjee, K. V. K. Reddy, Characterization of fully and partially penetrated Nd: YAG laser-weld dissimilar metal joints, Journal of Mechanical Science and Technology 32 (2), 2018, 615-621

[15] C. Douglas, Montgomery, Design and analysis of Experiments, John Wiley & sons Inc, New Work, 2009, pp. 13–19, and pp. 365–372

[16] Michael J. Crawley, The R- Book, John Wiley & Sons, Inc., New York, 2007.

[17] M. Pouranvari, P. Marashi, and M. Goodarzi, "Failure mode of dissimilar resistance spot welds between austenitic stainless and low carbon steels," 17th Int. Metall. Mater. Conf. Met. 2008 - Proc., pp. 3–8, 2008.